

# ~~A one year comparison~~ An assessment of 482-MHz radar wind profiler, RS92-SGP Radiosonde and the performance of a 1.5 $\mu\text{m}$ Doppler Lidar lidar for operational vertical wind measurements profiling based on a one-year trial

Eileen Päschke<sup>1</sup>, Ronny Leinweber<sup>1</sup>, and Volker Lehmann<sup>1</sup>

<sup>1</sup>DWD, Meteorologisches Observatorium Lindenberg-Richard Aßmann Observatorium

Correspondence to: Eileen Päschke  
(eileen.paeschke@dwd.de)

**Abstract.** We present the results of a one-year quasi-operational testing of the 1.5  $\mu\text{m}$  StreamLine Doppler lidar developed by Halo Photonics from 02 October 2012 to 02 October 2013. The system was configured to continuously perform a velocity-azimuth display (VAD)-scan pattern using 24 azimuthal directions with a constant beam elevation angle of ~~75°~~ 75°. Radial wind estimates were selected using a rather conservative signal-to-noise ratio (SNR)-based threshold of ~~-18.2 dB (0.015)~~ -18.2 dB (0.015). A 30 minute average profile of the wind vector was calculated based on the assumption of a horizontally homogeneous wind field through a ~~singular-value-decomposed~~ Moore-Penrose pseudoinverse of the overdetermined linear system. A strategy for ~~a~~ the quality control of the retrieved wind vector components is outlined ~~which is used to ensure for ensuring~~ consistency between the ~~retrieved winds and the assumptions inherent to the employed Doppler lidar wind products and the inherent assumptions employed in the~~ wind vector retrieval. ~~Finally, the lidar measurements are compared with operational~~ Quality-controlled lidar measurements were compared with independent reference data from a collocated ~~482-MHz operational~~ 482 MHz radar wind profiler running in a four-beam Doppler beam swinging (~~DBS~~) mode and winds from operational radiosonde measurements. The ~~intercomparisons show that intercomparison results reveal a particularly good agreement between~~ the Doppler lidar ~~is a reliable system for operational wind measurements in the atmospheric boundary layer (ABL) and the radar wind profiler, with root mean square errors ranging between~~ 0.5 m s<sup>-1</sup> and 0.7 m s<sup>-1</sup> for wind speed and between 5° and 10° for wind direction. The median of the half-hourly averaged wind speed for the intercomparison data set is

8.2 m s<sup>-1</sup>, with a lower quartile of 5.4 m s<sup>-1</sup> and an upper quartile of 11.6 m s<sup>-1</sup>.

## 1 Introduction

The wind field is one of the most important atmospheric parameters. Its accurate measurement with a high spatial and temporal resolution is crucial for operational Numerical Weather Prediction (NWP) models and it is ~~of course~~, of course, also vital for numerous other applications. The operational remote sensing of the vertical wind profile is ~~currently~~ dominated by radar wind profilers (RWP), with frequencies ranging from L-band to VHF. Here, the letter codes L and VHF (Very High Frequency) are standard band designations according to the IEEE standard radar-frequency letter-band nomenclature (Skolnik, 2001). The typical time resolution for wind profiles provided to NWP is currently 30 min.

Recently, a new generation of portable infrared (IR) Doppler ~~Lidar~~ lidar (DL) systems based on fiber-optic technology developed for the telecommunications industry has become commercially available. In contrast to conventional DL designs based on free-space optics, the use of fiber-optic elements considerably simplifies fabrication, alignment and long-term stability. While there is currently a large market demand for such systems from the renewable energy sector, it is also interesting to test the capabilities of these new instruments for possible future operational boundary layer wind profiling, complementary to radar profilers.

In particular, the DL may have the potential to measure winds below the height of the first range gate of low - UHF

RWP, which is typically on the order of a few hundred meters (about 450 m for the 482 MHz RWP used in this study). This RWP blind zone is due to the constraint of measuring in the far-field of the antenna and finite receiver recovery time. The overlap region between RWP and DL data provides a convenient option for cross-technology calibrations and consistency checks. Finally, the higher vertical resolution of DL data is particularly adequate for wind measurements in the lowest part of the boundary layer.

Previous intercomparisons of DL and RWP winds have generally shown good agreements (Cohn and Goodrich, 2002; Pearson et al., 2009; Shaw et al., 2003). These intercomparisons, however, were always based on temporally short-term measurement periods. For example, Cohn and Goodrich (2002) have shown from a measurement period of 2.3 h that the differences of the Doppler velocities obtained with a 915-MHz boundary layer RWP and the NOAA High Resolution Doppler Lidar (HRDL) had a standard deviation of about  $\sigma_r = 0.20 - 0.23 \text{ m s}^{-1}$ , which was attributed to turbulent variability and instrumental noise. A translation of this error into the corresponding error for the horizontal wind resulted in an error of less than  $0.11 - 0.27 \text{ m s}^{-1}$  for a 30-min measurement period, depending on the beam pointing sequence (five-beam or three-beam pointing DBS-Doppler beam swinging (DBS) configuration). Pearson et al. (2009) compared wind measurements from a 9 min Doppler lidar scan and radar data from a 10-min average 10 min averaged 1290 MHz radar data for four different times which also showed very good level of agreement, except for somewhat less well correlated wind speed data, which was attributed to insects or ground clutter contamination of the radar velocity data. A month long field study has been carried out in the Salt Lake Valley (Shaw et al., 2003). Here wind measurements have been collected with a 915 MHz RWP and a pulsed DL ( $\lambda = 10.59 \mu\text{m}$ ). Comparisons of half-hour consensus winds obtained with the RWP with corresponding VAD-winds from DL using a velocity-azimuth display (VAD) scan pattern showed broad agreement albeit considerable scatter, which was attributed to the different sampling volumes of the two systems.

The article describes the setup and methodology of the test, with a focus on aspects of data processing based on the systems direct output and the results of the comparison statistics derived from about 17.000 wind profiles that have been obtained over the course of a year. To the author's knowledge, such long time comparisons between Doppler lidar and radar wind profiler have not been done so far and thus may give valuable and more representative insights into the performance of Doppler lidar wind measurements. The paper is structured as follows: In Sect. 2 information describing the data set used for the analysis are given is described. It includes detailed information related to instrumentation and, above all, the details of the data processing and quality control. In Sect. 3 the statistics of one year

long DL measurements are discussed in comparison to RWP and radiosonde (RS) measurements. An interesting type of "gross error" due to a range ambiguity effect is discussed in Sect. 4. Finally, Sect. 5 presents a summary of the results and conclusions.

## 2 Data set

The intercomparison period used for our analysis is from 02 October 2012 to 02 October 2013. The wind data were collected data used for this analysis were obtained at the Lindenberg Meteorological Observatory - Richard Aßmann Observatory (RAO) - MOL-RAO) from 02 October 2012 to 02 October 2013. At this site RWP and radiosonde, RWP and RS winds are routinely measured and provided for assimilation into a number of NWP models. Since September 2012, a 1.5  $\mu\text{m}$  DL is being tested with regard to the efficient allocation of the focus of the capabilities of this measurement system for operational wind profiling within the atmospheric boundary layer (ABL). With a spatial separation of only about 30 m the installation of the DL was as close as possible to the RWP. These circumstances create outstanding conditions for the instruments intercomparison. Further informations on the single measurement systems are given below to achieve the best possible collocation for the intercomparison. Additionally, four routine radiosonde ascents are carried out on a daily basis with the launch site being about 500 m away from the remote sensing field site. This provides another independent data set of upper-air wind measurements. Obviously, the in-situ sampling characteristics of the radiosonde leads to non-optimal collocation and temporal matching for individual data points. Nevertheless, the capability of having three fully independent systems for vertical wind profiling is rather unique.

### 2.1 Instrumentation overview

In the following, a short description of the measuring principles set-up and some technical aspects for each of the instruments used is provided.

#### 2.1.1 1.5 $\mu\text{m}$ Doppler Lidar

The DL emits laser pulses in the near infrared which scatter off particles suspended in the atmosphere, like such as aerosols and clouds. Data availability is therefore linked to the presence of such particles. The backscattered light has a Doppler shift due to the movement of these particles which can be detected by optical heterodyning in the receiver. Assuming that the target is following the wind, the horizontal wind vector can be determined from the measured line-of-sight (LOS) Doppler wind values. The technical specifications of the StreamLine Doppler lidar developed by Halo Photonics are listed in Table ?? . The PRF value is 1. The pulse

repetition frequency (PRF) implies a maximum unambiguous range of about 10 km. For wind measurements, a VAD scan pattern was set-up as illustrated in Fig.1. The sketch is limited to  $n = 12$  beam pointing directions or rays, however, the measurement scan pattern was using  $n = 24$  azimuthal positions with a constant elevation angle  $\epsilon = 75^\circ$ . Measurements of Doppler velocities  $v_r(R, \alpha, t)$  were thus made along a circle at  $15^\circ$  constant intervals of azimuth  $\alpha$ .  $R$  indicates the range of the measurement, i.e. the distance of the backscattering volume along LOS, and  $t$  denotes the time of the measurement. For each of the 24 rays a total of 75000 laser shots have been emitted. The dwell time for one ray was about 5 seconds. Taking the time for the scanner to move movement into account, one full scan lasted about 3 minutes. For  $\epsilon = 75^\circ$ , the range gate length of  $\Delta R = 48 \text{ m}$  translates to a vertical resolution of about  $\Delta Z = 46 \text{ m}$ .

### 2.1.2 482 MHz radar wind profiler

While the measurement principle of the RWP is also based on the Doppler effect, the significantly longer wavelength of 62 cm makes it possible to obtain measurable echoes from both the particle-free (clear) atmosphere due to fluctuations of the refractive index as well as from the particle-laden atmosphere (clouds with sufficiently large particles and precipitation), see e.g. Gossard and Strauch (1983); Gage et al. (1999). Therefore, wind information can almost always be obtained for the entire depth of the troposphere provided the refractive index fluctuations have a sufficient strength at half the radar wavelength.

The passive phased array antenna of the system is designed to steer the beam into five different directions (vertical and four obliques with an elevation angle of  $74.8^\circ$ ). In the operational configuration, the RWP cycles continuously through the four oblique beam directions. The operational set-up uses two different pulse widths to obtain data with different radial resolutions (low and high mode). Eventually, a total of five cycles per mode is used to generate 30 min averaged profiles. The averaging algorithm used is called "consensus averaging" (Fischler and Bolles, 1981; Strauch et al., 1984) and is applied to each beam direction separately. This algorithm facilitates discrimination between "good" and "bad" estimates in the low SNR regime regime of low signal-to-noise ratios (SNR) (Frehlich and Yadlowsky, 1994). For the purpose of this study, only data from the low mode with a pulse width of  $\tau = 1000 \text{ ns}$  are considered. RWP low mode measurements are available for a total of 96 range gates extending from 450 m up to 9380 m. The radial and the vertical resolution of one range gate is  $\Delta R = 150 \text{ m}$  and  $\Delta Z = 145 \text{ m}$ , respectively. The vertical spacing of the range gates due to oversampling with 650 ns is 94 m. A summary of the technical specifications of the 482 MHz RWP is given in Table ??1.

### 2.1.3 RS92-SGP Radiosonder radiosonde

The Vaisala RS92 radiosonde measures vertical profiles of pressure, temperature, and humidity from the ground up to the balloon bursting altitude limit of approximately 40 km. To retrieve the horizontal and meridional winds ( $u, v$ ) based on the change of the sonde position, the RS92 is equipped with a GPS receiver. The noise in the raw  $u$  and  $v$  winds due to the radiosonde's pendulum-like motion and the noise of the GPS data is reduced by a low-pass digital filter (Dirksen et al., 2014). At Lindenberg, radiosondes are routinely launched four times a day at standard times (00, 06, 12, and 18 UTC). The temporal resolution of the sounding wind data is of 40 s, the typical ascent rate of about  $5 \text{ m s}^{-1}$  leads to a vertical resolution of about 200 m.

## 2.2 Doppler lidar data processing

The system output quantities relevant for the wind vector retrieval are the estimates of Doppler velocity  $V_r(R, \alpha, t)$ , where subscript  $i$  indicates the  $i$ 'th azimuth measurement within one VAD scan,  $V_r(R, \alpha, t)$ , and the corresponding signal-to-noise ratio  $SNR = S/N$ , where  $S$  is the average signal power and  $N$  the average noise power (Frehlich and Yadlowsky, 1994). The wind analysis is based on the following steps of data processing: (i) employment of SNR threshold technique SNR-based thresholding for sorting out "bad" (noise affected) Doppler estimates from "good" estimates, (ii) calculation of 30 min average Doppler Lidar lidar VAD scans to match the temporal resolution of the RWP measurements, (iii) reconstruction of the three vector components  $u, v, w$ , (iv) quality check to ensure consistency of retrieved winds and all the assumptions used in order to calculate  $u, v, w$  and (v) interpolation of the three vector components from the "Doppler lidar grid" to the "Wind profiler grid" to generate achieve the spatial matching. The latter step, however, is relevant for the final only necessary for the comparison between DL and RWP measurements and which otherwise would not have been necessary. Further details on the above-described processing steps will be outlined below.

### 2.2.1 SNR thresholding technique

The measurable detector signal current in a DL is clearly affected by noise effects, mainly dominated by shot noise from the local oscillator (Frehlich and Kavaya, 1991; Frehlich, 1996). Since the systems operate down to very low SNR conditions, this leads to the occurrence of outliers in the signal properties estimation process ("bad" estimates), which are usually uniformly distributed in frequency over the Nyquist-limited search band (Dabas, 1999). In order to separate between "good" (reliable) and "bad" (unreliable) estimates, a simple SNR-based SNR-based thresholding tech-

nique is a common approach. Depending on the **instrument-** **s-instruments'** specific parameters the SNR threshold may vary between different instruments. There are a number of studies focusing on techniques for the determination of reasonable threshold **SNR**, e.g. Frehlich and Yadlowsky (1994); Dabas (1999). For reliable Doppler velocity estimates with **a-an approximate** precision of  $< 30 \text{ cm s}^{-1}$  the manufacturer of the StreamLine Doppler lidar suggests **a threshold-SNR using a threshold SNR** of -18.2 dB (0.015). **From test measurements during stable atmospheric conditions (vertical velocity close to zero), however, it turns out that this is-** see also Fig. 2 c in Pearson et al. (2009). **Note that this precision value describes the performance of the Doppler estimator which depends on both the instrument (detector noise) and the natural atmospheric variability within the resolution volume. In order to investigate this threshold two test measurements were made in quiescent atmospheric conditions using a permanent vertical stare configuration. To the extent that it is possible to assume zero atmospheric vertical motion for these cases, the uncertainty in the Doppler estimates is only due to instrumental (noise) effects. The data from these tests reveal that the suggested threshold is apparently a rather conservative value-which is significantly-choice thereby limiting our data availability-** In Fig. 2 the Doppler velocities measured during this test period are plotted against the corresponding value for **SNR +1 (intensity the parameter "intensity" (SNR + 1, a numerically more convenient quantity))**. For the range  $0.992 < (SNR + 1) < 1.006$   $0.992 < (SNR + 1) < 1.006$  the Doppler velocities are uniformly distributed over the search band **indicating a relatively high fraction which corresponds to the expected statistical distribution of "bad" estimates. Between the outer edge (SNR + 1 = 1.006) of the band of uniformly distributed Doppler and the proposed SNR threshold (SNR + 1 = 1.015), however, there is a large gap so that by employing this threshold SNR a huge amount of Beyond the suggested threshold of 1.015, the Doppler values clustered around zero Hertz are distributed as expected for "good" measurements-are discarded estimates. The difference between the obvious structural change of the frequency distribution at about 1.008 and the actual threshold of 1.015 is an indication for the possibility to lower the SNR-threshold without risking a significant increase of "bad" estimates.** Tests have shown, for instance, that the decrease of the threshold SNR from -18.2 dB (0.015) down to -20 dB (0.010) would increase the data availability by almost 40 %. However, since the goal of this paper was to assess the accuracy of strictly quality controlled DL wind measurements with respect to the RWP, a refinement of the SNR thresholding technique is left for a future study.

## 2.2.2 Calculation of 30 min averaged VAD scans

For the intercomparison of winds from the DL and the RWP it is necessary to achieve a match of the temporal resolution

between both systems. The DL winds were therefore averaged to 30 min, which corresponds to the operational configuration of the RWP. Two different routes are available for this averaging: One option is to reconstruct first the cartesian vector components  $u, v, w$  from each single VAD scan which takes about 3 min (see also Sect. 2.1.1) and then to calculate averaged  $u, v, w$  vector components from **the** ten full VAD scans. The other options is to **average all VAD scans first and then to reconstruct create mean VAD scans by averaging the ten radial velocity measurements for each azimuth and then reconstructing** the  $u, v, w$  wind vector components from **these averaged VAD scans this single average scan**. Here the second way was used since it corresponds best to the "consensus averaging" method employed in the RWP processing.

## 2.2.3 Wind vector retrieval

The 3D wind vector profiles are determined on the basis of the 30 min averaged VAD scans **describe-described** above. Each averaged VAD scan includes temporally averaged Doppler velocities for **the** 24 different **azimuth** directions. In principle, **radial** measurements in three linearly independent **direction-directions** would be sufficient for a 3D wind vector reconstruction. **In this and the following sections (see Sect. 2.2.4), however, However,** it will be shown that the use of VAD scans with more than three directions brings considerable benefits in terms of error minimization and in terms **for conducting quality assurance of conducting quality checks** of the reconstructed 3D wind vector components, i.e.  $u, v, w$ .

(i) *Least squares wind components  $u, v, w$  using SVD:*

Assuming a stationary and horizontally homogeneous wind field, i.e.  $\mathbf{v}(x, y, z, t) \sim \mathbf{v}(z)$ , the three wind vector components  $u, v$  and  $w$  can be obtained by solving the overdetermined linear system

$$A \mathbf{v} = \mathbf{V}_r \quad , \quad (1)$$

where  $\mathbf{v} = (u \ v \ w)^T$ ,  $\mathbf{V}_r = (V_{r1} \ V_{r2} \ V_{r3} \ \dots \ V_{rn})^T$  (with  $n = 360^\circ/15^\circ = 24$   $n = 360^\circ/15^\circ = 24$ ). The rows of matrix  $A$  are comprised of the unit vectors along the  $n$  pointing directions (**rays** or rays) with azimuth  $\alpha_i, i = 1 \dots n$ , that is

$$A = \begin{pmatrix} \sin(\alpha_1) \sin(\phi) & \cos(\alpha_1) \sin(\phi) & \cos(\phi) \\ \sin(\alpha_2) \sin(\phi) & \cos(\alpha_2) \sin(\phi) & \cos(\phi) \\ \sin(\alpha_3) \sin(\phi) & \cos(\alpha_3) \sin(\phi) & \cos(\phi) \\ \dots & \dots & \dots \\ \sin(\alpha_n) \sin(\phi) & \cos(\alpha_n) \sin(\phi) & \cos(\phi) \end{pmatrix} \quad . \quad (2)$$

If the azimuth angle  $\alpha_i$  (with  $i = 1, \dots, n$ ) and the elevation angle  $\phi$  are chosen properly (see also Fig.1), matrix  $A$  is a nonsquare  $24 \times 3$  matrix with full column rank, **that is**  $\text{rank}(A) = 3$ . Equation (1) is clearly overdetermined and can be solved using the method of least squares. The solution

is exact when it does exist, otherwise only an approximate solution can be found. A least squares solution  $\mathbf{v}^*$  is obtained by minimizing the square of the residual in the 2-norm, i.e. by minimizing  $\|\mathbf{V}_r - A\mathbf{v}\|_2^2$  (e.g., Strang, 1993). In doing so the least squares solution is given by a standard square (3x3) system

$$A^T A \mathbf{v} = A^T \mathbf{V}_r \quad , \quad (3)$$

where  $A^T$  is the transpose of  $A$ . Since  $A$  has full column rank  $A^T A$  is positive definite and invertible, that is  $\mathbf{v}$  can be obtained by evaluating the normal equation

$$\mathbf{v} = (A^T A)^{-1} A^T \mathbf{V}_r = A^+ \mathbf{V}_r \quad , \quad (4)$$

where  $A^+$  denotes the Moore-Penrose Pseudoinverse of  $A$ . The normal equations (3), however, tend to worsen the condition of the matrix, i.e.  $\text{cond}(A^T A) = (\text{cond}(A))^2$ . For a large condition number, small errors in the (measured) data can produce large errors in the solution. The singular value decomposition (SVD) can be used to solve least squares problem without squaring the condition of the matrix. Employing the SVD, the matrix  $A$  is decomposed using the factorization

$$A = U D V^T \quad , \quad (5)$$

where  $U$  is an 24x24 orthogonal matrix,  $V$  is an 3x3 orthogonal matrix and  $D$  is an 24x3 diagonal matrix whose elements  $\sigma_i$  are called the singular values of  $A$ . Then a the least squares solution can be expressed as

$$\mathbf{v} = A^+ \mathbf{V}_r = V D^{-1} U^T \mathbf{V}_r \quad . \quad (6)$$

The advantage of using the SVD in the context of least squares minimization has also been discussed in Boccippio (1995).

#### (ii) Error propagation:

Assuming that the Doppler velocity vector  $\mathbf{V}_r$  has a corresponding known vector of uncertainty, i.e.  $\hat{\sigma}_e = (\sigma_{e1} \sigma_{e2} \sigma_{e3} \dots \sigma_{en})^T$ , the propagation of the radial velocity errors to error of the errors of the components of the wind vector  $\mathbf{v}$  can be calculated employing the error propagation law. In matrix form, this can be written as

$$C_{\mathbf{V}_r \mathbf{V}_r} = A C_{\mathbf{v} \mathbf{v}} A^T \quad (7)$$

or after rearranging to calculate the unknown uncertainties-

$$C_{\mathbf{v} \mathbf{v}} = A^{-1} C_{\mathbf{V}_r \mathbf{V}_r} (A^{-1})^T \quad , \quad (8)$$

where  $C_{\mathbf{V}_r \mathbf{V}_r}$  and  $C_{\mathbf{v} \mathbf{v}}$  denote the variance-covariance matrices of  $\mathbf{V}_r$  and  $\mathbf{v}$  defined through the diagonal nxn matrix

$$C_{\mathbf{V}_r \mathbf{V}_r} = \begin{pmatrix} \bar{\sigma}_{e1}^2 & 0 & \dots & 0 \\ 0 & \bar{\sigma}_{e2}^2 & \dots & 0 \\ \vdots & \vdots & \ddots & \vdots \\ 0 & 0 & \dots & \bar{\sigma}_{en}^2 \end{pmatrix} \quad (9)$$

and the 3x3 matrix

$$C_{\mathbf{v} \mathbf{v}} = \begin{pmatrix} \sigma_u^2 & \sigma_{uv} & \sigma_{uw} \\ \sigma_{vu} & \sigma_v^2 & \sigma_{vw} \\ \sigma_{wu} & \sigma_{wv} & \sigma_w^2 \end{pmatrix} \quad , \quad (10)$$

respectively. Here, the variance-covariance matrix  $C_{\mathbf{V}_r \mathbf{V}_r}$  is diagonal, because it is assumed that the errors of the  $n$  components of  $\mathbf{V}_r$  are independent in different directions (Cohn and Goodrich, 2002). It has further been assumed that variances in the elevation angle and azimuth angles occurring in  $A$  can be neglected. By evaluating the rhs of Eqn. (11) the random errors For a more detailed discussion of the derivation of the error propagation law in matrix form the reader is referred to Arras (1998), Tellinghuisen (2001) and Boccippio (1995).

The uncertainties  $\sigma_u$ ,  $\sigma_v$  and  $\sigma_w$  of the retrieval for  $u, v, w$  can be calculated from by evaluating the square roots of the diagonal elements of the variance-covariance matrix  $C_{\mathbf{v} \mathbf{v}}$ . For the more interested reader on the derivation of error propagation law in matrix form and its application reference is made to , and . Using again the notation of the Moore-Penrose pseudoinverse  $A^+$  of matrix  $A$  it is shown in App. A that rearranging terms in eqn. (7) yields

$$C_{\mathbf{v} \mathbf{v}} = A^+ C_{\mathbf{V}_r \mathbf{V}_r} (A^+)^T \quad . \quad (11)$$

In the least square problem described above the measured radial velocities for each beam direction have a precision of  $\sigma_{ei} < 30$  -  $\sigma_{ei} < 30$  cm s<sup>-1</sup> with  $i = 1, \dots, n$  (see Sect. 2.2). Taking error propagation into account one obtains a precision of  $\bar{\sigma}_{ei} < 10$  -  $\bar{\sigma}_{ei} < 10$  cm s<sup>-1</sup> for each beam direction from a full 30 min averaged VAD scan. Then, setting  $\bar{\sigma}_{e1} \equiv \dots \equiv \bar{\sigma}_{rn} \equiv \bar{\sigma}_e < 10$  -  $\bar{\sigma}_{e1} \equiv \dots \equiv \bar{\sigma}_{rn} \equiv \bar{\sigma}_e < 10$  cm s<sup>-1</sup> we find by evaluating eqn. (11) by means of SVD that

$$\text{diag } C_{\mathbf{v} \mathbf{v}} = (124.4 \underline{1.9510^{-6}} \underline{2.0110^{-7}} \underline{1.9510^{-6}}, 124.4 \underline{9.5510^{-7}} \underline{2.01410^{-7}}) \quad (12)$$

Eventually, calculating the square roots of the diagonal elements of  $C_{\mathbf{v} \mathbf{v}}$  yields

$$\sigma_u = \sigma_v < \underline{11.1511.15} \text{ cm.scm s}^{-1} \text{ and } \sigma_w < \underline{2.112.11} \text{ cm.scm s}^{-1} \quad , \quad (13)$$

which describes the propagation of the errors in the radial measurements to the wind vector components due to geometry. Note that this assumes the exact validity of eqn. (1), which means that the homogeneity assumption is exactly fulfilled. Possible effects of deviations from this assumption are discussed below.

Finally, the above described approach is used to study the variation of the retrieval uncertainties depending on the variation of the number of beam directions per VAD scan. Table 2

clearly shows that with increasing number of beam directions the uncertainties can be reduced, most obviously the uncertainty  $\sigma_w$  of the vertical wind component  $w$ . Thus it can be concluded, that a VAD scan is not only useful for horizontal wind vector reconstructions but also for the determination of the vertical wind provided the number of beam directions is high enough. Here, however, it should be kept in mind that the reconstructed  $w$  would differ from direct stare measurements because of the horizontal homogeneity assumption.

## 2.2.4 Quality assurance

The wind retrieval algorithm described in Sect. 2.2.3 is based on two assumptions. So far, the assumption of horizontal homogeneity has already been mentioned. This is a necessary assumption to devise a closed set of equations for the unknown wind vector components  $u, v, w$ . The employment of regression techniques to obtain estimates for  $u, v$  and  $w$  presumes linear independence of the data set used for the retrieval, additionally. Wind retrievals from routinely DL measurements are thus only valid, if the real atmospheric conditions and the measurements meet these assumptions. Furthermore, the retrieval through the pseudoinverse needs to be numerically stable, which is not always guaranteed when only a subset of radial measurements is available due to atmospheric variability in backscattering. In this section two parameters are described which have been used for conducting quality assurance of the retrieved winds.

### (i) Test of horizontal homogeneity

It is well known that the wind field is not always horizontally homogeneous (Goodrich et al., 2002; Cheong et al., 2008), this is mainly due to convection, gravity waves or shear induced turbulence. Characteristic temporal and spatial scales for turbulence are  $T = 10$  sec and  $L = 1$  m. For thermally induced convective processes we typically have  $T = 5$  min and  $L = 500$  m. Thus, with reference to a full DL scan lasting about 3 min and with a scanning circle having height dependent diameters  $d_C$  of about  $d_C \sim 300$  m at an altitude of  $\sim 550$  m and  $d_C \sim 5360$  m at  $\sim 10$  km it is often the case that due to the occurrence of turbulent motions there are rapid wind fluctuations along the scanning circle and accordingly the assumption of a horizontally homogeneous wind field is not fulfilled. For that reason 3D wind vector retrievals based on measurements collected during such inhomogeneous wind field conditions have to be flagged. The strategy used to identify wind retrievals during such inhomogeneous wind field conditions is described next.

For a horizontally homogeneous wind field, the reconstruction of the mean wind  $u, v, w$  from radial velocities obtained by a VAD scan scheme can be regarded as a sine wave fitting (Banakh and Smalikho, 2013). The overall quality of the fit to this sine wave model is affected by deviations from

these homogeneous conditions and can be measured by the coefficient of determination  $R^2$  defined through

$$R^2 = 1 - \frac{\sum_i (V_{ri} - \tilde{V}_{ri})^2}{\sum_i (V_{ri} - \bar{V}_r)^2}, \quad (14)$$

with  $\bar{V}_r = \sum_i V_{ri}$  and  $\tilde{V}_{ri}$  denoting the radial velocities from the "sine wave fit".  $R^2$  is used as a quality control parameter for  $u, v$  and  $w$  reconstructions.

For the analysis in the present paper a reconstructed 3D wind vector has been rejected if  $R^2 < 0.95$ . An interpretation of this value is that 95 % of the variations of the averaged VAD scan Doppler velocities are due to variations in the beam direction  $\alpha_i$  and only 5% of the variations have to be explained by other factors. For an exact horizontally homogeneous wind field and exact Doppler velocity estimates the VAD Doppler velocity variations are solely caused by the variation in the beam direction  $\alpha_i$ . Thus, with the requirement  $R^2 < 0.95$  it is possible to identify such VAD scans for which the assumption of a horizontal wind field is only partially fulfilled. It is important to point out that the selection of  $R^2 < 0.95$  as a strict data rejection threshold is only based on our experiences and therefore ad-hoc. Further work is required to investigate whether homogeneity can be restored in the statistical sense by judicious temporal averaging.

### (ii) Collinearity diagnostics

Following the strategy described above it was found, however, that  $R^2 \geq 0.95$  can only be regarded as a necessary condition for 'good' reconstructions. A sufficient condition is that wind vector reconstructions, since the retrieval needs also to be numerically stable with respect to small errors in the input or, in other words, well-conditioned. This is achieved when the degree of collinearity among the Doppler velocity measurements used for the retrieval is relatively weak, since a robust linear independence of the sampling directions is an essential prerequisite for the reconstruction of the wind vector. Multicollinearity describes a high linear relationship among one or more independent variables (Belsley et al., 1980) and it is also a well known issue in regression analysis that multicollinearity may result in parameter estimates with incorrect signs and implausible magnitudes (Mela and Kopalle, 2002) or may affect the regressions robustness, i.e. small changes in the data may result in large changes in the parameter estimates (Boccippio, 1995). Thus, multicollinearity makes the parameter estimates less reliable and has to be detected to exclude erroneous (unphysical)  $u, v, w$  retrievals from VAD scans. In the context of least squares parameter estimation from a VAD scan, a high degree of multicollinearity may occur in situations when there are large azimuthal gaps in the measurements due to limited or non-existing backscattering targets within the atmosphere. Then, one measured Doppler velocity

can be linearly predicted from the neighboring values and thus the available measurements from such an "incomplete" scan contain redundant information on the wind field and it becomes difficult or impossible to distinguish their individual influences on the  $u, v$  and  $w$  estimates. This issue was already recognized by Matejka and Srivastava (1991) from in the VAD analysis of single-Doppler Radar radar Data.

The condition number  $CN$  is a parameter that can be used for the detection of collinearity. If the condition number of the problem is small (close to 1) the degree of collinearity is relatively weak. In contrast, a large condition number is an indicator for a strong collinearity among the variables. Boccippio (1995) employed the condition number for an analysis of the VVP (volume velocity processing) retrieval method and identified condition numbers around 9–12 as a threshold indicating collinearity in the regression. In Wissmann et al. (2007) values for  $CN$  of 10 and 30 are mentioned to indicate medium and serious degrees of multicollinearity, respectively.

For the collinearity diagnostics the approach as described in Boccippio (1995) has been adopted. In particular,  $CN$  is calculated based on the standardized (scaled) data matrix  $Z = AS$ , where

$$S = \text{diag}(s_1, s_2, s_3) \quad \text{with} \quad s_i = (A_i^T A_i)^{-1/2} \quad (15)$$

Here,  $A_i$  denote the columns of matrix  $A$ , i.e.  $A = [A_1 \ A_2 \ A_3]$ . If the singular value decomposition of  $Z$  is used, the condition number  $CN(Z)$  can be calculated as

$$CN(Z) = \frac{\eta_{max}}{\eta_{min}}, \quad (16)$$

where  $\eta_i$  ( $i = 1, 2, 3$ ) are the singular values of  $Z$ . The standardization of the data matrix is recommended by Belsley (1991). For further details concerning the scaling problem of the condition number it is also the reader is referred to Wissmann et al. (2007). Fig. 3 indicates an increase of the condition number with increasing azimuthal gaps for a VAD scan configuration. For a gap size of 270–280 deg the condition number is  $CN = 30$  which according to Wissmann et al. (2007) indicates severe collinearity. In such a case, all radial measurements stem from only one quadrant of the scan. Geometrically it is obvious that the linear independence in this case is numerically weak. For the quality control used in the present analysis a  $CN$  threshold of 10 has been used which. This means that 3D wind vector reconstructions obtained from VAD scans with azimuthal gaps  $\geq 240$  degrees have been rejected. Future work is required to investigate to what extent this rather conservative threshold can be relaxed.

### (iii) Example

An example for the outcome of the above described strategy of quality control is illustrated in Fig. 4. The 30 min averaged wind profiles shown here are based on DL measurements from 22.08.2013, which was a typical summer day

with a pronounced diurnal cycle of a convective boundary layer (CBL). The upper left and right plots show unverified 30 min plots on the left show 30 min averaged vertical profiles of wind speed and wind direction, respectively. The lower plots estimated from eqn. (6). The plots on the right show the corresponding wind profiles after additional consistency checking. The parameters  $R^2$  and  $CN$  for each of the retrievals are shown in Fig. 5. The processing was done as described in Sec. 2.2.3. Appendix ?? provides guidance for the calculation of wind speed and wind direction from  $u, v, w$  retrievals, additionally. It can be observed that profiles between 8:00 UTC+2:00 and 14:00 UTC+2:00 were rejected. This is mainly due to values for  $R^2 < 0.95$   $R^2 < 0.95$  which can be attributed to the inhomogeneous flow occurring within a well established CBL. Figure 6 illustrates this situation by showing VAD fits for both homogeneous and inhomogeneous situations.

With regard to the condition number, Fig. 5 shows only a few cases with  $CN > 10$ , most  $CN > 10$ , mostly in the upper part of the boundary layer where azimuthal gaps within the VAD scan are more likely due to absence of backscattering targets a low particle density. Even if multicollinearity is a rare problem there is a need to define a  $CN$  threshold (here  $CN > 10$ ) as a sufficient condition. This can be motivated based on the examples shown  $CN > 10$  as an additional condition. An instructive example to illustrate this need is given in Fig. 7. Three 4, which shows three mean VAD scans obtained between 11:03 UTC and 11:32 UTC for three adjacent range gate heights at  $h_1 = 1460, 48$  m,  $h_2 = 1506, 84$  m and  $h_3 = 1553, 21$  m are shown  $h_1 = 1460, 48$  m,  $h_2 = 1506, 84$  m and  $h_3 = 1553, 21$  m along with the corresponding consistency check parameters  $R^2$  and  $CN$ . Obviously, it is noticeable, that the sine wave fit at  $h_3$   $h_3$  has a much greater amplitude compared to  $h_2$  and  $h_1$   $h_2$  and  $h_1$ . Since the amplitude is a measure for the wind speed, this would imply much stronger winds at  $h_3$   $h_3$  than at the lower heights at  $h_2$  and  $h_1$ . The condition number of  $CN = 22$   $h_2$  and  $h_1$ . This data point corresponds to the "red pixel" at the height gate of 1553.21 m in Fig. 4. Obviously, this wind is implausible. A detailed analysis of the mean VAD-scan indicates that the sine-wave fit of the radial measurements is nearly perfect in this case, with  $R^2 = 0.98$ , see Fig. 7. However, radial wind data are only available in five almost contiguous directions which are only spanning a sector of 75°, namely from 315° to 30° in azimuth. Equivalently, this leaves an azimuthal gap of 285° where no radial winds are available. In general it seems to be possible that a valid wind vector can also be retrieved in this setting, however even small errors in the radials are obviously amplified up to the point where the end result is grossly in error. The condition number of  $CN = 22$  clearly reflects the large gap of radial velocity measurements between the azimuth angles 50° and 300°. The high degree of collinearity among the Doppler velocities for this VAD-scan is obviously leading

to erroneous magnitudes for the parameter estimates  $u$ ,  $v$  and  $w$ .

In summary, the parameters  $R^2$  and  $CN$  turn out to be useful quality control indicators for the 3D wind vector retrieval although they apparently do not detect all “bad” winds. In figure 4 the plot of rather large gap in the quality flagged wind speed still includes in 12th position a profile whose values does not seem to fit into the overall wind speed pattern despite the good quality check parameters  $R^2 = 0.98$  and  $CN = 3$ . It remains for future work to analyse the error sources for this type of possibly wrong wind retrieval radial velocity measurements and the high degree of collinearity for this VAD scan.

### 2.2.5 Regridding Data preparation for intercomparisons

The Doppler lidar measurements obtained with our configurations have a vertically finer resolution than the measurements of the RWP. For the purpose of intercomparisons between Doppler lidar-, RWP and radiosonde measurements it is therefore useful to define a common reference grid to make the values comparable. Since the interpolation from a coarser grid to a finer grid is naturally more problematic than vice versa, we have chosen the wind radar grid as the reference grid for our studies. For the interpolation of the 30-min-30 min averaged 3D wind vector components  $u$ ,  $v$ ,  $w$  from the finer Doppler lidar (or finer Radiosonde) grid to the coarser and equidistant grid of the RWP, a cubic spline interpolation was used. In detail this means that between two grid points of the finer grid we first determined a smooth function is determined first, which passes exactly through those points. Between two grid points of the finer grid, the this smooth function is evaluated at the coarser grid point to get the interpolated value. The procedure achieves the vertical matching of the profiles required for the intercomparison. However, the horizontal separation of the RS profile due to the wind-induced drift of the in-situ sensor has not been taken into account. This introduces an error of representativity as an additional contribution to the RS-DL differences. For the mean ascent rate of the RS, the top of the ABL is typically reached after less than 10 minutes. For a mean wind speed of  $10 \text{ m s}^{-1}$  this leads to a maximal horizontal separation of only 6 km. It is assumed that the representativity difference due to this horizontal separation of sampling volumes is tolerable, however a refined study can certainly use the sondes GPS position for an additionally stratification of the data set. With respect to temporal matching, each of the profiles is assigned to a uniform UTC based time grid.

## 3 Analysis/Statistics

In this section the statistics of one-year long DL measurements for wind speed and wind direction is presented. A guidance for the calculation of wind speed and direction from the  $u, v, w$  retrievals is provided in App. ??. The results are verified with corresponding measurements obtained with a collocated 482 MHz RWP and measurements from RS92-SGP Radiosonde launched at the same observation site.

### 3.1 Data availability

For the period under investigation, the maximum number of 30 min averaged profiles for wind speed and wind direction wind profiles is 17568 provided the measurement conditions are perfect, i.e. occurrence of aerosols and/or cloud droplets at any time and any height during the year of measurements. in terms of optical conditions (clouds and aerosols) and wind field structure (homogeneous vs. non-homogeneous). Clearly, measurement conditions are not always ideal as shown in Fig. 8 which naturally leads to a decrease in the number of quality controlled data. At the lowest level of the reference grid (i.e. 552 m) a total of 9798 ( $\sim 56\%$ ) averaged values could be obtained whereas these numbers decrease to 697 ( $\sim 4\%$ ) at 2056 m. The decrease of data availability continues further upwards and approaches less than 10 ( $\sim 0.06\%$ ) for altitudes higher than 7038 m. This strong decrease of data availability reflects the nature of the with height reflects the vertical distribution of aerosol and cloud particle concentration particles within the atmosphere. This is the main reason why the IR Doppler lidar is mainly used for wind measurements within the ABL. Of course, these limitations of DL data availability need to be taken into account for the generation of a representative wind climatology.

Also shown in Fig. 8 is the data availability obtained with the collocated RWP (low mode) and those from routine RS launches. Not surprisingly, both measurement systems provide higher data availabilities within the free atmosphere than the DL. The decrease of RWP data availability with height is related to the profile of the structure constant of refractive index turbulence ( $C_n^2$ ) which can be observed almost continuously in the lower atmosphere (Atlas, 1990). For the two comparisons, i.e. Doppler lidar-DL vs. RWP (hereafter referred to as DLWR) and Doppler lidar vs. radiosonde-DL vs. RS (hereafter referred to as DLRS), we only use the subset where valid data are available from both systems, i.e. the intersection of the respective data sets. Figure 8 gives an overview to what extent this further decreases the data availability for our statistical analysis. To get almost representative statistical results for a ‘one-year comparison’ the comparisons are restricted to heights up to  $\sim 2800$  m for the comparison DLWR and up to  $\sim 1300$  m for the comparison DLRS, which guarantees that

the sample size is  $> 200$ . For this data basis the precision  $\Delta \bar{v}_{speed}$  of a calculated quasi-annual wind speed is on the order of about  $\Delta \bar{v}_{speed} = 7e-4 \text{ m s}^{-1}$  (see also App. ??).  $\Delta \bar{v}_{speed} = 7e-4 \text{ m s}^{-1}$ .

### 3.2 DLWR and DLRS Comparisons

The calculated statistics in this section serves as a diagnostics to get insights into the validity of the 3D wind vector retrievals from DL measurements. Abbreviations used for the error scores are: ME (mean error), MAE (mean absolute error) and RMSE (root mean squared error).

#### 3.2.1 Scatterplots

For a first overview, the 30 min averaged lidar winds are compared against 30 min averaged RWP winds on the one hand and against temporally consistent matched radiosonde winds on the other hand for the full period and all heights. The corresponding scatter plots are shown in Fig. 9 for wind speed and wind direction, respectively. Regarding the wind speed it can be observed that for both comparisons (DLWR and DLRS) a great fraction of the data sets falls on the majority of data points falls very close to the identity line which indicates a general good agreement of the respective data samples. In more detail, however, the correlation ( $m$ ) indicates a slight slightly better linear relationship between radiosonde and Doppler lidar RS and DL wind speeds ( $m = 0.99$ ) than between RWP and Doppler lidar DL wind speeds ( $m = 0.97$ ). This seems to be mainly due to better agreements of higher wind speeds (e.g.  $> 20 \text{ m/s}$ ) for the DLRS comparison than for the DLWR comparison.

Additionally we observe a greater spread of data pairs around the identity line is observed for the DLWR comparison than for the DLRS comparison. However, the respective RMSE scores which measure the average magnitude of the error indicate better agreement for the DLWR comparison than for the DLRS comparison. Since the RMSE gives a high weight to large errors, the lower RMSE value for the DLWR comparison also indicates that the largest differences occur between the Doppler Lidar and Radiosonde lidar and radiosonde data. Regarding the wind direction the dots of a huge number of data pairs are concentrated around the identity line and thus likewise indicate good agreements for both comparisons. However, the dots of some minor a small fraction of data pairs are somewhat widely spread and indicate a weak weaker relationship between measured wind directions. We also find that this observation is more pronounced for the DLWR comparison than for the DLRS comparison. Note that the clustered data points around  $360^\circ$  at both the horizontal and vertical axis are due to the eye lie azimuth range  $2\pi$ -periodicity of azimuth.

A general

#### 3.2.2 Annual mean wind profiles

A good agreement in the statistics of Doppler Lidar, Radar Wind Profiler and Radiosonde Doppler lidar, radar wind profiler and radiosonde measurements is also reflected in the annual mean of the measured vertical profiles for wind speed and direction shown in Fig. 10. To quantify the errors, the following verification scores are analyzed: Mean error (ME), mean absolute error (MAE) and root mean squared error (RMSE).

Regarding the DLWR comparison the ME for the wind speed changes a little in sign with varying height up to about 1800 m, whereas the range of speed variations is from  $-0.2 \text{ m/s} < \text{ME} < 0.3 \text{ m/s}$ . Above 1800 m the ME is always positive and increases from  $\sim 0 \text{ m/s}$  at 1800 m up to  $0.2 \text{ m/s}$  at about 2500 m. Thus, assuming that the RWP measures the 'truth' a systematic error using the RWP measurements as a reference a systematic difference indicating a slight overestimation of Doppler Lidar DL wind speeds can be identified for altitudes higher than 1800 m. The reason for this difference is unclear. It is probably also justified to take the possibility of a small range dependent bias in the RWP data into account, which could be further investigated with a long-term RWP-RS intercomparison. Additionally, a sign change of ME is observed for height below 1800 m in both the DLWR and DLRS comparisons. This small effect is likely due to a hardware issue in the DL that was unfortunately only detected and fixed after the campaign. Concerning the annual mean wind direction there is in general also good agreement between DL and RWP measurements. Here the mean differences mostly vary between  $\pm 1$  deg. For With regard to the error scores MAE and RMSE, the DL and RWP measurements agree in wind speeds mostly within a range of about  $0.3 \text{ m/s} < \text{MAE} < 0.5 \text{ m/s}$  and  $0.5 \text{ m/s} < \text{RMSE} < 0.7 \text{ m/s}$ . For the wind direction  $3 \text{ deg} < \text{MAE} < 4 \text{ deg}$  and  $5 \text{ deg} < \text{RMSE} < 10 \text{ deg}$ . The small differences between the MAE and RMSE ranges for the wind speed additionally indicate that there is some variation in the magnitude of the errors but large errors can be ruled out in all likelihood. This is in contrast to the slightly larger differences between the MAE and RMSE ranges for the wind direction at low range gate heights, suggesting that here larger errors occur.

Regarding the DLRS comparison we observe a smaller bias ( $-0.2 \text{ m/s} < \text{ME} < 0.1 \text{ m/s}$ ) ( $-0.2 \text{ m/s} < \text{ME} < 0.1 \text{ m/s}$ ) below 1500 m than in the DLWR comparison. The verification scores MAE and RMSE, however, are somewhat larger, i.e.  $0.5 \text{ m/s} < \text{MAE} < 0.7 \text{ m/s}$  and  $0.7 \text{ m/s} < \text{RMSE} < 0.9 \text{ m/s}$  for wind speed and  $5 \text{ deg} < \text{MAE} < 6 \text{ deg}$  and  $9 \text{ deg} < \text{RMSE} < 12 \text{ deg}$  for wind direction.

The presented long-term intercomparison results confirm the main findings of previous intercomparison results (see Sect. 1) Sect. 1) obtained from short-term measurement pe-

riods. The good agreement also indicates a rather small instrument error of all systems, since the methodology of the comparison was targeted at minimizing the sampling error by minimizing of both the temporal and spatial separation (about 30 m) between the Doppler lidar and the radar wind profiler.

#### 4 Range aliasing effects for smaller SNR thresholds

In Sect. 2.2.1 it has already been mentioned that the SNR threshold of -18.2 dB (0.015) used for the analysis in the present paper (0.015) is a rather conservative threshold, with the consequence that a huge amount of "good" estimates are rejected. It can therefore be assumed that smaller SNR thresholds can possibly also be used. An analysis of the Doppler lidar measurements based on an SNR threshold  $< 1.015 \text{ SNR-threshold} < 0.015$  revealed an interesting type of "gross error", which was not observed employing the conservative SNR threshold  $= 1.015 \text{ SNR-threshold} = 0.015$ . In radar meteorology, this type of "gross error" is already well known as range ambiguity (or range aliasing). Range aliasing occurs if there are atmospheric backscattering targets at altitudes  $> Z_{max}$ , where  $Z_{max}$  defines the greatest unambiguous measurement height specified through  $Z_{max}$  defines the maximum unambiguous range determined by the pulse repetition frequency (PRF) via  $PRF_{max} = c/(2Z_{max})$ . Here,  $c$  defines the speed of light. In such a case an incorrect calculation of  $c$  via  $PRF_{max} = c/(2Z_{max})$  is stronger than the backscattering in the equivalent unambiguous height range.

In such cases, the range of the backscattering target is unavoidable, since the received echo and the outgoing pulse are assigned to each other incorrectly: The received signal is incorrectly assigned. The received echo is not associated with the pulse just transmitted, but with the pulse transmitted prior to the latest one. The wind profiles shown in previous Fig. 12 give an example where such range aliasing effects have been gives an illustrative example of such a range aliasing effect in the DL data, which could be uniquely detected by comparing Doppler lidar measurements with RWP measurements. Shown are DL and RWP (high and low mode) wind profiles for three different times (11:00, 11:30 and 12:00 UTC). The low mode (higher resolution) profile of the RWP covers a height range from about 500 m up to about 7 km, whereas the high mode (lower resolution) profile provides data between 4 and 13 km height. Both modes have a sufficient low PRF to avoid range aliasing under all practical circumstances. The DL profiles in contrast are limited to the height range below about 1 km. The striking feature in the DL data are the strong northerly winds (in excess of  $50 \text{ m s}^{-1}$ ) which are clearly erroneous in this height band. These are due to second-trip echoes originating from

heights of around 11 km which are incorrectly assigned to the height of about 1 km. Note that the maximum unambiguous range of 10 km in the DL is due to the PRF of 15 kHz.

It is important to point out that such "gross errors" can be easily circumvented by changing the PRF in the sense that the maximum unambiguous sampling range is increased. Of course, this also reduces the number of pulses that can be averaged in a given time interval. While this has a slightly negative effect on the performance of the lidar, the avoidance of gross errors due to range-aliasing clearly outweighs the associated minor disadvantage, at least in operational settings.

## 5 Conclusions

The capability of a new generation of portable IR Doppler Lidars systems for future operational boundary layer wind profiling, complementary to radar profilers, has been tested. For this purpose, one year long times series of horizontal wind vector retrievals from Doppler lidar and radar wind profiler measurements of Doppler velocity have been compared mainly for atmospheric boundary layer heights between

The signal-to-noise ratio threshold of -18.2 dB (0.015) for reliable Doppler wind estimates with a precision of  $500 \text{ m} < 30 \text{ cm s}^{-1}$  and 2800 m. These interval limits coincide with the lower limit for 482 MHz wind profiler measurements and an upper limit up to which nearly continuous Doppler lidar measurements were possible. The higher limit is a representative value for the RAO site and is subject to natural conditions as the atmospheric aerosol loading at this site. There is a general good agreement in the measurement statistics of both systems and thus confirms previous studies on this issue but on the basis of a much smaller data collection. These results strengthen the basic idea to use DL measurements below 500 m to fill the gap below 500 m in the wind profiles where 482 MHz RWP wind measurements are no more possible.

The underlying was chosen in a very conservative way.

For the usually employed assumption of a horizontally homogeneous wind field within the volume sampled by the lidar, a methodology was developed for the retrieval of the wind vector from a velocity-azimuth display sampling configuration using 24 azimuthal directions with a constant elevation of  $75^\circ$ . The assumptions used for the 3D wind vector retrievals from Doppler velocity measurements have been generally the same for both systems. A huge advantage of the Doppler Lidar, however, is that lidar is the full hemispheric scanning capability of the DL. This allows for more flexible sampling strategies than the RWP which is in contrast to most radar profilers, which are restricted to measurements using the DBS mode. In this context it became apparent that DL measurements based on a VAD

sean with  $n = 24$  beam directions enable additional quality checks to ensure consistency of retrieved winds and retrieval assumptions Doppler beam swinging mode.

Quality control methods were derived and implemented for testing of the homogeneity assumption used in the retrieval, as well as for the sensitivity of the retrieval against small errors in the input data. In particular, if the number of measurement directions ( $n$ ) is large enough, the "Goodness-of-fit" parameter quantified by  $R^2$  turned out to be a useful tool to determine the degree of homogeneity of the wind field during the time at which measurement data have been collected. Inhomogeneous. Clearly, non-homogeneous wind fields are more characteristic frequently found within the atmospheric boundary layer than in the free atmosphere. That is why such a consistency check is more important for wind retrievals within which renders this test quite important for operational wind profiling with the Doppler lidar.

A second test of a robust linear independence among the Doppler velocity measurements by means of the condition number  $CN$  turned out to be useful for detecting erroneous wind estimates which have their origin in a high sensitivity of the retrieval with respect to input errors, a situation which occurs in the case of large measurement gaps within a single VAD scan. This is observed when the backscattering targets are not equally distributed within the VAD-sampled volume, a condition which frequently occurs within the transition zone from the atmospheric boundary layer into the boundary layer than in the free atmosphere. The

Especially the  $R^2$  quality test employed discards with the employed threshold of  $R^2 < 0.95$  for bad retrievals discards 7568 profiles of 17.568 maximum possible profiles over the year, a considerable proportion of DL wind retrievals when the wind field is non-homogeneous. This is Doppler lidar wind retrievals. This was justified because the focus of the investigation was the evaluation of the Doppler lidar accuracy based on strictly quality controlled wind measurements of the DL. By the same token, the SNR threshold was also chosen in a very conservative way. It remains. However, it remains an important topic for future work to find out to what extent these constraints both the threshold for  $R^2$  as well as the threshold for the SNR can be relaxed for the sake of a higher data availability without compromising the data quality of the measurements. A further test of linear independence among the Doppler velocity measurements by means of the condition number  $CN$  turned out to be useful to detect physically implausible retrievals which may have its origin in large measurement gaps within a single VAD scan. This can be the case if the backscattering targets are inhomogeneously distributed which frequently occurs within the transition zone from the atmospheric boundary layer into the free atmosphere. The results of the

Using the processing methodology outlined in the paper, one year long times series of 30 min averaged horizontal wind vector retrievals were calculated from the Doppler lidar and compared with operational radar wind profiler

measurements in the atmospheric boundary layer at heights between 500 m and 2800 m. These interval limits are determined by the lowest height gate of the 482 MHz wind profiler and the height up to which a sufficient number of Doppler lidar measurements could be obtained to allow for a stable intercomparison statistics. This upper height limit is mainly determined by the natural atmospheric aerosol loading at Lindenberg.

There is a very good agreement in the measurements of both systems, which confirms previous studies that were made on the basis of a much smaller data collection. These results strengthen the basic idea to use DL measurements below 500 m to fill the gap where 482 MHz RWP wind measurements are no more possible. It is obvious that the strict employment of the two test parameters  $R^2$  and  $CN$  presented in this study make clear the importance of quality assurance testing and it is understood that the strategy of quality assurance testing employed here  $CN$  was important for the good agreements between Doppler lidar and radar wind profiler measurements.

*Acknowledgements.* This work was carried out as part of the HD(CP)<sup>2</sup> project (sub-project: "O1 - supersites") funded by the German Federal Ministry of Education and research (BMBF) - grant number 01LK1209E. The authors would like to acknowledge METEK GmbH for its support during the installation and use of the "StreamLine" Doppler Lidar lidar system. We are also grateful to Guy Pearson for comments on an earlier version of the manuscript.

The service charges for this open access publication have been covered by Deutscher Wetterdienst (DWD).

## Appendix A: Error propagation law

If  $n > 3$  matrix  $A$  is not invertible. Multiplying eqn. (7) from the left by  $A^T$  and inverting subsequently the expression  $(A^T A)$  one obtains

$$(A^T A)^{-1} A^T C_{\mathbf{v}_r, \mathbf{v}_r} = A^+ C_{\mathbf{v}_r, \mathbf{v}_r} = C_{\mathbf{v}_v} A^T, \quad (\text{A1})$$

where  $A^+$  denotes the Moore-Penrose pseudoinverse of  $A$  (see also eqn. (4)). Next, multiplying with  $A$  from the right yields

$$A^+ C_{\mathbf{v}_r, \mathbf{v}_r} A = C_{\mathbf{v}_v} A^T A, \quad (\text{A2})$$

and inversion of  $(A^T A)$  gives

$$A^+ C_{\mathbf{v}_r, \mathbf{v}_r} A (A^T A)^{-1} = C_{\mathbf{v}_v}. \quad (\text{A3})$$

It remains to show that  $A(A^T A)^{-1} = (A^+)^T$ . First, using the substitution  $G = (A^T A)^{-1}$  one can write

$$(A^+)^T = (GA^T)^T. \quad (\text{A4})$$

With  $(BC)^T = C^T B^T$  and  $(D^T)^T = D$  (properties of transpose) one can also write

$$(A^+)^T = (A^T)^T G^T = AG^T, \quad (\text{A5})$$

and re-substitution yields

$$(A^+)^T = A((A^T A)^{-1})^T. \quad (A6)$$

1065 Making use of  $(D^T)^{-1} = (D^{-1})^T$  gives

$$(A^+)^T = A((A^T A)^T)^{-1}, \quad (A7)$$

and repeated use of the properties of transpose, yields

$$(A^+)^T = A(A^T(A^T)^T)^{-1} = A(A^T A)^{-1}. \quad (A8)_{1125}$$

## References

- 1070 Arras, K. O.: An Introduction To Error Propagation: Deriva-<sub>1130</sub>  
tion, Meaning and Examples of Equation  $C_Y = F_X C_X F_X^T$ ,  
ETH-Zürich, Technical Report No. EPFL-ASL-TR-98-01 R3,  
doi:10.3929/ethz-a-010113668, (last access: 11 november 2014),  
1998.
- 1075 Atlas, D.: Radar in Meteorology, American Meteorological Society,<sub>1135</sub>  
45 Beacon Street, Boston, MA 02176, 1990.
- Banakh, V. and Smalikhov, I.: Coherent Doppler Wind Lidars in a  
Turbulent Atmosphere, Artech House Publishers, 2013.
- Belsley, D.: A guide to using the collinearity diagnostics, Computer  
1080 Science in Economics and Management, 4, 33–50, 1991. <sub>1140</sub>
- Belsley, D., Kuh, E., and Welsch, R. E.: Regression Diagnostics:  
Identifying Influential Data and Sources of Collinearity, John  
Wiley & Sons, Inc., Hoboken, New Jersey, 1980.
- Boccippio, D. J.: A Diagnostic Analysis of the VVP Single-Doppler  
1085 Retrieval Technique, J. Atmos. Oceanic Technol., 12, 230–248,<sub>1145</sub>  
doi:10.1175/1520-0426(1995)012<0230:ADAOTV>2.0.CO;2,  
1995.
- Cheong, B. L., Palmer, R. D., Yu, T.-Y., Yang, K.-F., Hoffman,  
M. W., Frasier, S. J., and Lopez-Dekker, F. J.: Effects of Wind  
1090 Field Inhomogeneities on Doppler Beam Swinging Revealed by  
an Imaging Radar, J. Atmos. Oceanic Technol., 25, 1414–1422,  
doi:10.1175/2007JTECHA969.1, 2008.
- Cohn, S. A. and Goodrich, R. K.: Radar Wind Profiler Radial Ve-  
1095 locity: A Comparison with Doppler Lidar, J. Appl. Meteor., 41,  
1277–1282, 2002. <sub>1155</sub>
- Dabas, A.: Semiempirical Model for the Reliability  
of a Matched Filter Frequency Estimator for  
Doppler Lidar, J. Atmos. Oceanic Technol., 16, 19–28,  
doi:10.1175/1520-0426(1999)016<0019:SMFTRO>2.0.CO;2,  
1100 1999. <sub>1160</sub>
- Dirksen, R. J., Sommer, M., Immler, F. J., Hurst, D. F., Kivi,  
R., and Vömel, H.: Reference quality upper-air measure-  
ments: GRUAN data processing for the Vaisala RS92 radi-  
1105 osonde, Atmospheric Measurement Techniques, 7, 4463–4490,  
doi:10.5194/amt-7-4463-2014, 2014.
- Fischler, M. A. and Bolles, R. C.: Random Sample Consensus: A  
Paradigm for Model Fitting with Applications to Image Analysis  
and Automated Cartography, Commun. Assoc. Comput. Mach.,  
24, 381–395, 1981.
- 1110 Frehlich, R.: Simulation of Coherent Doppler Li-  
dar Performance in the Weak-Signal Regime,  
J. Atmos. Oceanic Technol., 13, 646–658,  
doi:10.1175/1520-0426(1996)013<0646:SOCDLP>2.0.CO;2,  
1996.
- 1115 Frehlich, R. and Yadlowsky, M.: Performance of Mean-Frequency  
Estimators for Doppler Radar and Lidar, J. Atmos. Oceanic Tech-  
nol., 11, 1217–1230, 1994.
- Frehlich, R. G. and Kavaya, M. J.: Coherent laser radar perfor-  
mance for general atmospheric refractive turbulence, Appl. Opt.,  
30, 5325–5352, doi:10.1364/AO.30.005325, 1991.
- 1120 Gage, K. S., Williams, C. R., Ecklund, W. L., and John-  
ston, P. E.: Use of Two Profilers during MCTEX for  
Unambiguous Identification of Bragg Scattering and  
Rayleigh Scattering, J. Atmos. Sci., 56, 3679–3691,  
doi:10.1175/1520-0469(1999)056<3679:UOTPDM>2.0.CO;2,  
1999.
- Goodrich, R. K., Morse, C. S., Cornman, L. B., and Cohn,  
S. A.: A Horizontal Wind and Wind Confidence Algorithm for  
Doppler Wind Profilers, J. Atmos. Oceanic Technol., 19, 257–  
273, doi:10.1175/1520-0426-19.3.257, 2002.
- Gossard, E. E. and Strauch, R. G.: Radar Observations of Clear Air  
and Clouds, Elsevier, 1983.
- Matejka, T. and Srivastava, R. C.: An Improved Version of  
the Extended Velocity-Azimuth Display Analysis of Single-  
Doppler Radar Data, J. Atmos. Oceanic Technol., 8, 453–466,  
doi:10.1175/1520-0426(1991)008<0453:AIVOTE>2.0.CO;2,  
1991.
- Mela, C. and Kopalle, P.: The impact of collinearity on regression  
analysis: The asymmetric effect of negative and positive correla-  
tions, Applied Economics, 34, 667–677, 2002.
- Pearson, G., Davies, F., and Collier, C.: An Analysis of the Per-  
formance of the UFAM Pulsed Doppler Lidar for Observing  
the Boundary Layer, J. Atmos. Oceanic Technol., 26, 240–250,  
doi:10.1175/2008JTECHA1128.1, 2009.
- Shaw, W., Darby, L., and Banta, R.: A comparison of winds  
measured by a 915 MHz wind profiling radar and a Doppler  
lidar, 83rd AMS annual meeting (12th Symp. on Met. Ob-  
serv. & Instrument.), Long Beach, CA, 9–13 February, P1.8,  
https://ams.confex.com/ams/pdfpapers/58646.pdf, 2003.
- Skolnik, M. I.: Introduction to Radar Systems, McGraw-Hill, 2001.
- Strang, G.: The Fundamental Theorem of Linear Algebra, The  
American Mathematical Monthly, 100, 848–855, 1993.
- Strauch, R. G., Merritt, D. A., Moran, K. P., Earnshaw, K. B., and  
van de Kamp, D.: The Colorado wind profiling network, J. At-  
mos. Oceanic Technol., 1, 37–49, 1984.
- Tellinghuisen, J.: Statistical Error Propagation, J. Phys. Chem. A,  
105, 3917–3921, doi:10.1021/jp003484u, 2001.
- Wissmann, M., Toutenburg, H., and Shalabh: Role of Cate-  
gorical Variables in Multicollinearity in the Linear Re-  
gression Model, Department of Statistics, University Mu-  
nich, Germany, Technical Report Number 008, 34 pp.,  
http://nbn-resolving.de/urn/resolver.pl?urn=nbn:de:bvb:19-epub-2081-0,  
last access: 11 november 2014, 2007.

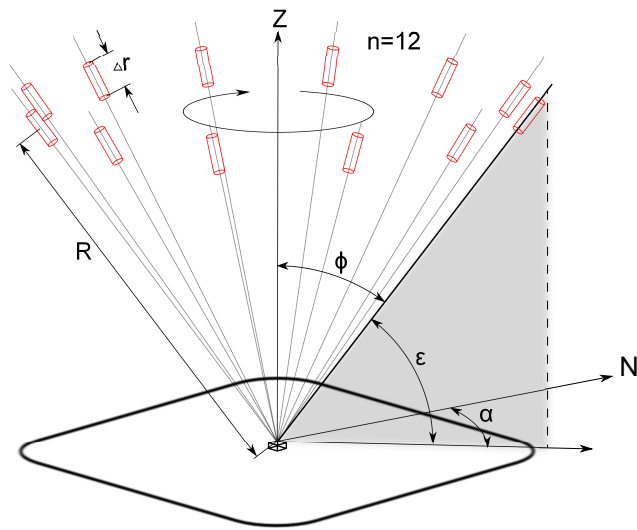


**Figure 1.** Example for a velocity-azimuth display (VAD) scanning technique for  $n = 12$  beam directions. The laser beam of the Doppler Lidar points upwards with a constant elevation angle  $\epsilon$  and rotates around the vertical  $Z$  with configurable azimuth angles  $\alpha$ . The red volumes symbolize an emitted "light"-disturbance of a specified period of time (i.e. pulse width  $\Delta t$ ) travelling along the line-of-sight (LOS).  $R$  is the range of the measurement along LOS and  $\Delta r$  defines the pulse length. The latter is related to the pulse width via  $\Delta r = c * \Delta t / 2$ , with  $c$  denoting the speed of light.

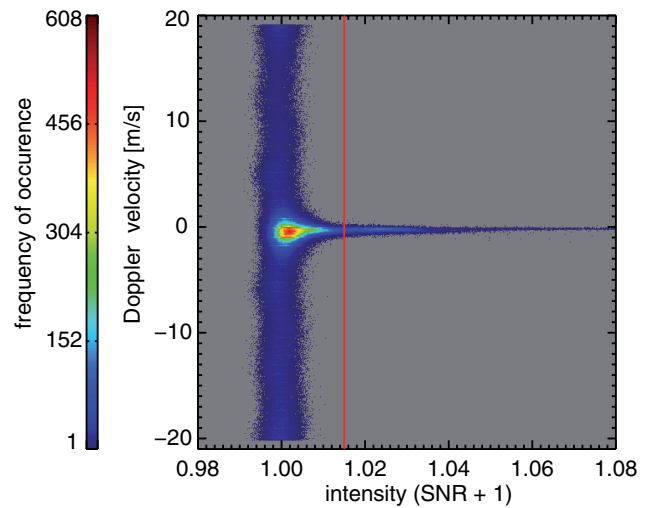


**Figure 2.** Intensity ( $SNR + 1$ ) vs. Doppler velocity plot based on Doppler lidar measurements from two measurement different time periods during stable atmospheric conditions (0600–0700 UTC 2013-07-05–6–7 UTC 2013-07-05 and 0700–0800 UTC 2013-07-22–8 UTC 2013-07-22) with which were characterized by quiescent atmospheric conditions, indicated by vertical velocities close to zero. The used Doppler lidar configuration was STARE, i.e. a continuous vertically pointing laser beam. For the range  $0.992 < (SNR + 1) < 1.006$  the Doppler velocities are uniformly distributed over the search band ( $\pm 19.4 \text{ ms}^{-1} \pm 19.4 \text{ ms}^{-1}$ ) indicating a relatively high fraction of "bad" estimates. For  $SNR + 1 \geq 1.006$  the Doppler lidar delivers plausible values ("good" estimates). The red line indicates the SNR-threshold  $(SNR + 1) = 1.015$  used for the data analysis in the present paper.

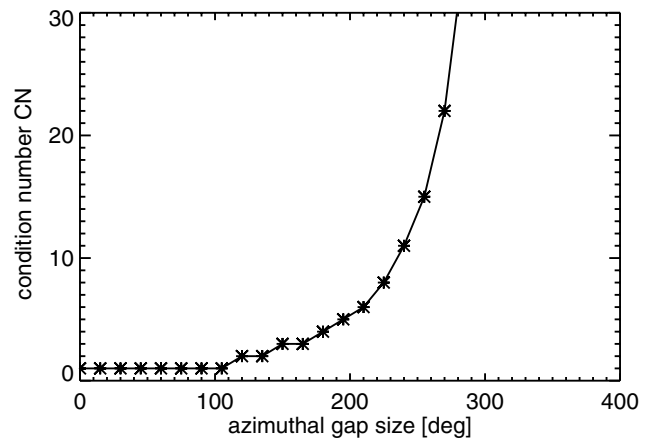


**Figure 3.** Condition number (CN) vs. azimuthal gap size for a VAD scan with  $15^\circ$  intervals of azimuth  $\alpha$  and a constant elevation angle  $\epsilon = 75^\circ$ .

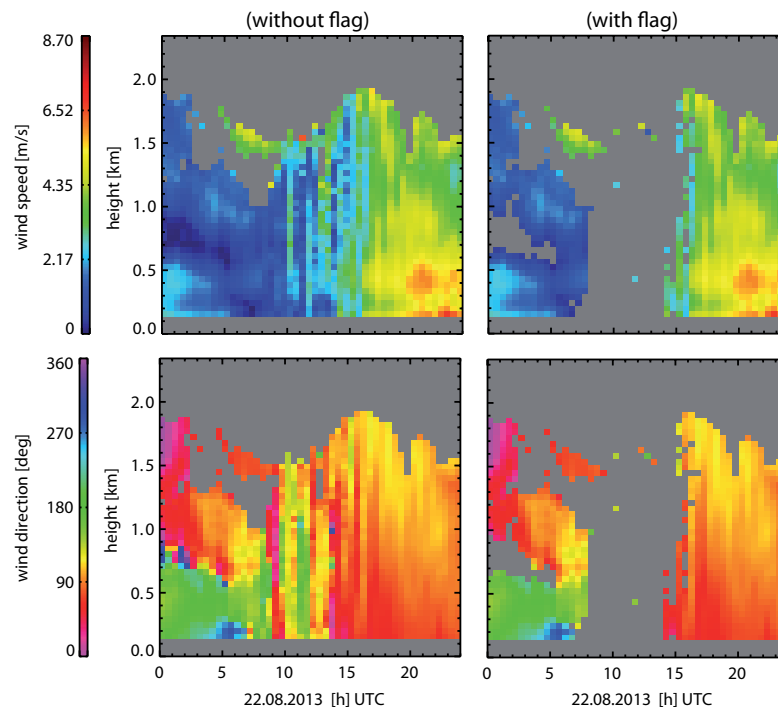


**Figure 4.** Left column: Example for non-quality assured wind profile retrievals (top: wind speed, bottom: wind direction) from Doppler lidar measurements for a typical summer day (2013-08-22). Each profile represents a 30 min average of VAD Doppler Lidar measurements with one scan lasting about 3 minutes. Right column: Same wind retrievals as shown in the left column but where profiles with test parameters  $R^2 < 0.95$  and  $CN > 10$  have been discarded.

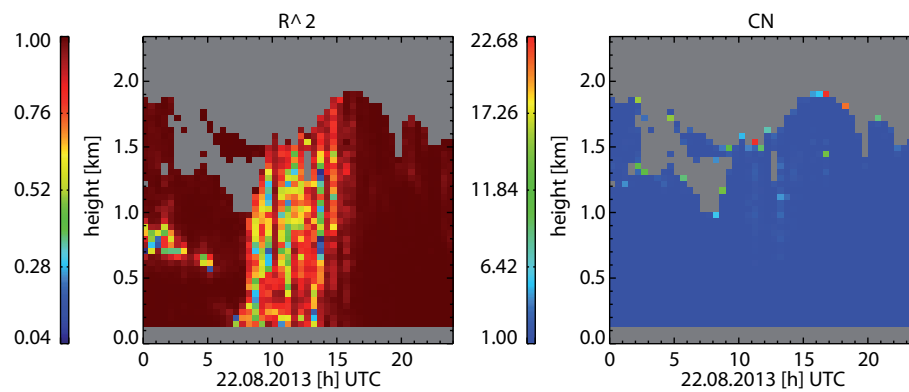


**Figure 5.** Calculated quality control parameters for the wind profiles shown in Fig. 4.  $R^2$  is the coefficient of determination which provides a measure for the "goodness" of sine wave fit into the VAD Doppler velocity measurements. To ensure that the horizontal homogeneity assumption inherent to the wind vector retrieval is fulfilled, wind vector reconstructions with  $R^2 < 0.95$  are classified as non reliable. Additionally, retrievals with  $R^2 \geq 0.95$  are only valid for a condition number  $CN \leq 10$ . The latter ensures a moderate degree of collinearity within the VAD scan Doppler velocity measurements.

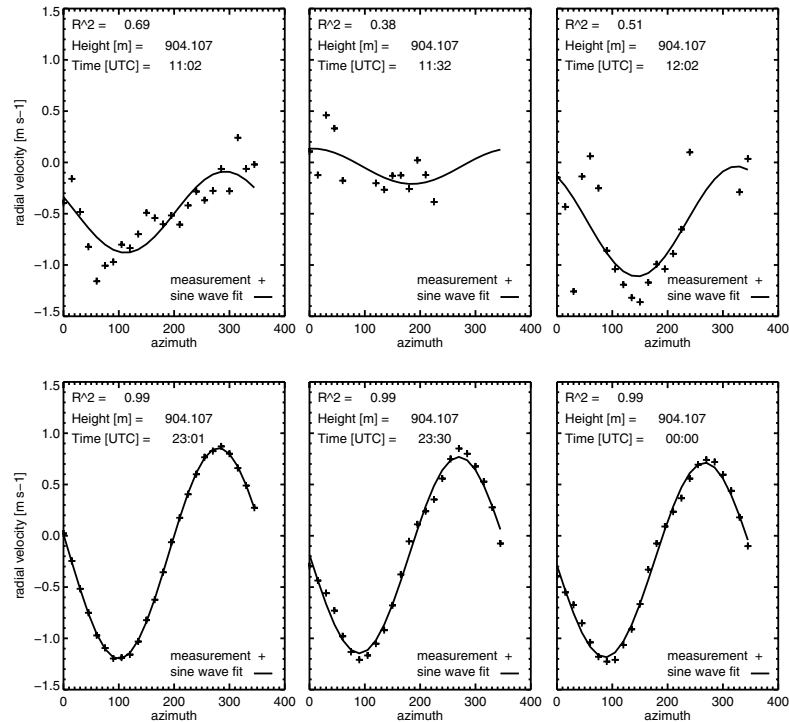


**Figure 6.** Examples for single sine wave fits into 30 min averaged VAD scans used to reconstruct the 30 min averaged wind profiles shown in Fig. 4 at 904 m height with the time stamps 11:02 UTC, 11:32 UTC and 12:02 UTC (upper row) and the three time stamps 23:01 UTC, 23:30 UTC and 0:00 UTC (lower row). The measurements in the upper line have been obtained during a well evolved CBL where horizontal homogeneous conditions are not met and which is also reflected in the low  $R^2$  values. The measurements in the lower row have been obtained during stable atmospheric conditions at night. Here, the high values for  $R^2$  indicate that the assumption of a horizontally homogeneous wind field is better fulfilled.

**Table 1.** Parameters of the HALO Photonics "Streamline" Doppler Lidar and the Vaisala/Rohde&Schwarz 482 MHz wind profiler (LAP-16000) installed at the observation site RAO. During the measurement period from 02 October 2012 to 02 October 2013 the two operating parameters (1) total number of pulses averaged and (2) resolution of Doppler velocity have been changed. The values in the brackets are valid starting from 26 July 2013. [The wind profiler values for range spacing and dwell time are valid for the "low mode".](#)

	Doppler lidar	Radar wind profiler
wavelength	1.5 $\mu\text{m}$	62 cm
pulse width	160 ns	1000 ns
range gate length	48 m	94 m
<a href="#">first gate</a>	<a href="#">90 m</a>	<a href="#">450 m</a>
points per range gate	16	1
total number of range gates	200	96
total number of pulses averaged	75000	507904 (491520)
resolution of Doppler velocity	$\pm 0.0382 \text{ m s}^{-1}$	0.1195 (0.1250)
telescope focus	800 m	not applicable
pulse length	25 m	150 m
total observation time per range gate	320 ns	-
<a href="#">range spacing</a>	-	650 ns
sampling frequency	50 MHz	1.538 MHz
<a href="#">dwell time</a>	<a href="#">5 s</a>	<a href="#">41.65 s</a>
Nyquist velocity	$\pm 19.4 \text{ m s}^{-1}$	30.586 (31.996) $\text{m s}^{-1}$
number of FFT points	1024	512
pulse repetition frequency	15 kHz	12.195 (12.346) kHz

**Table 2.** Decrease of the uncertainties ( $\sigma_u, \sigma_v, \sigma_w$ ) in the 3D wind vector component retrievals  $u, v$  and  $w$  with increasing number  $n$  of equidistant beam directions per VAD-scan. The values are calculated via Eqn. (11) assuming a Doppler velocity uncertainty of  $\sigma_r = 10 \text{ cm s}^{-1}$   $\sigma_r = 10 \text{ cm s}^{-1}$  for each beam direction.  $\Delta\alpha$  indicates the azimuth resolution.

n	$\Delta\alpha$ [deg]	$\sigma_u = \sigma_v$		$\sigma_w$	
		<del><math>[m s^{-1}]</math></del>	$[cm s^{-1}]$	<del><math>[m s^{-1}]</math></del>	$[cm s^{-1}]$
3	120		31.5470		5.97717
4	90		27.3205		5.17638
6	60		22.3071		4.22650
12	30		15.7735		2.98858
18	20		12.8790		2.44017
24	15		11.1536		2.11325
36	10		9.10684		1.72546

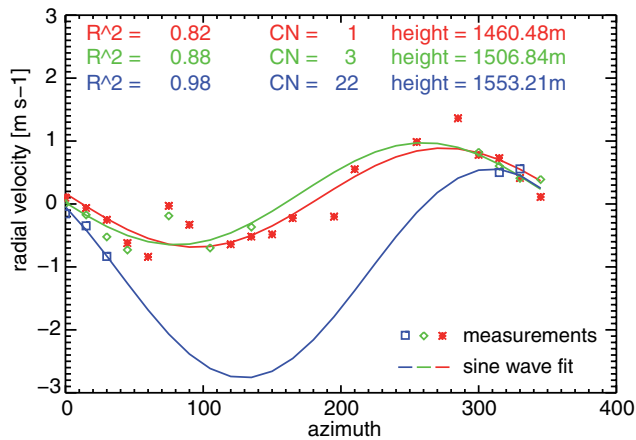


**Figure 7.** Examples for three sine wave fits used to reconstruct the 30 min averaged wind profiles shown in Fig. 4 at the three adjacent heights  $h_1=1460.48\text{ m}$ ,  $h_2=1506.84\text{ m}$  and  $h_3=1553.21\text{ m}$  for the single time stamp 12:02 UTC. Additionally for each fit the quality control parameters  $R^2$  and  $CN$  are also given. The sine wave fit at  $h_3$  has a high  $R^2$  but due to the large azimuthal gap size within the measurements the condition number  $CN$  is relatively high indicating a high degree of multicollinearity. The latter results in implausible magnitudes of the wind speed yielding unphysical vertical gradients in the wind speed profile shown in Fig. 4 at the time stamp 12:02 UTC).

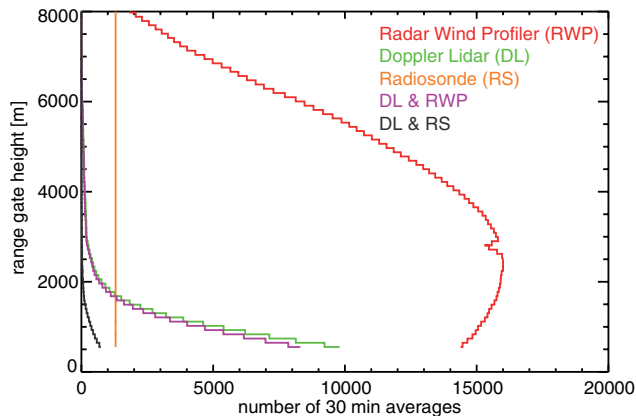


**Figure 8.** Overview of the data availability from one year measurements with Doppler Lidar (DL), Radar Wind Profiler (RWP) and Radiosonde (RS). Data availability refers to 30 min averaged profiles for wind speed and direction. The number of data used for the DLWR comparison is a subset of data indicated by DL & RWP where both systems provide valid data at the same time. The graph denoted with DL & RS reflects a subset of data where the DL and RS provide valid data at the same time and which have been used for the DLRS comparison.

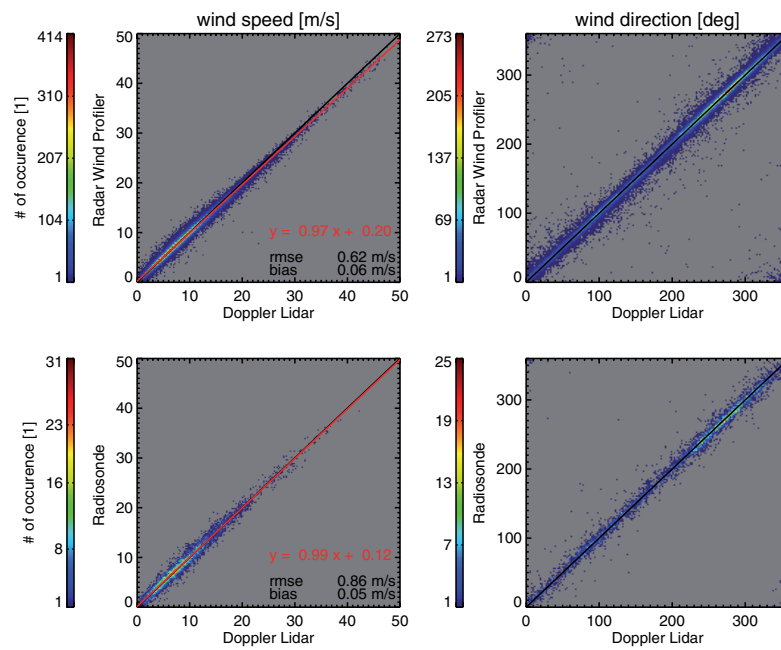


**Figure 9.** top: Scatter plots of one-year 30 min averaged horizontal wind speed and direction from Doppler Lidar and 482 MHz Radar radar Wind Profiler measurements (DLWR) bottom: Scatter plots of one-year 30 min averaged horizontal wind speed and direction from Doppler lidar and Radiosonde (DLRS). top and bottom: In principle all The scatter plots include measurements from all heights. The red line indicates the identity line.

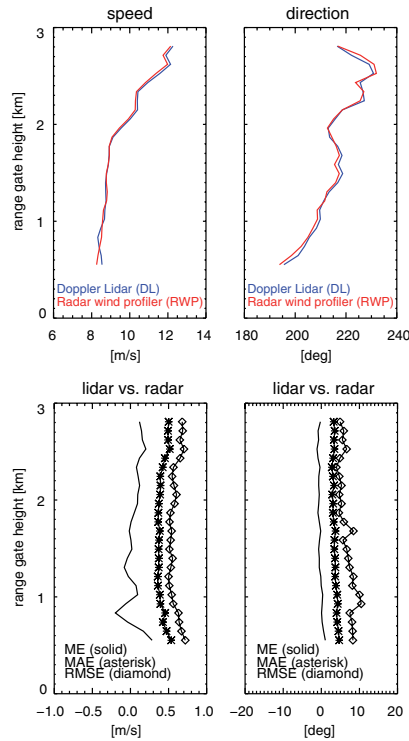


**Figure 10.** Statistical results of the DLWR comparison. The upper two panels show the annual mean of wind speed and direction obtained from Doppler Lidar and Wind profiler measurements, respectively. Error bars denoting the precision of the wind speeds in the annual profiles are not shown because of its very low magnitudes (see also the remarks in Sect. 3.1). The lower two panels show the respective verification scores ME (mean error), MAE (mean absolute errors) and RMSE (root mean squared error).

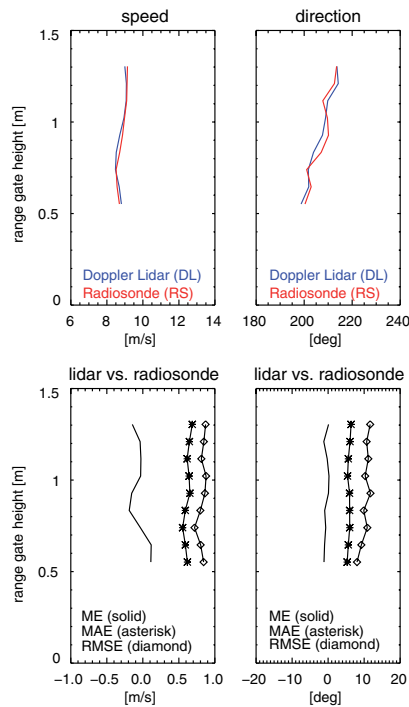


**Figure 11.** Same as in Fig. 10 but for the DLRS comparison.

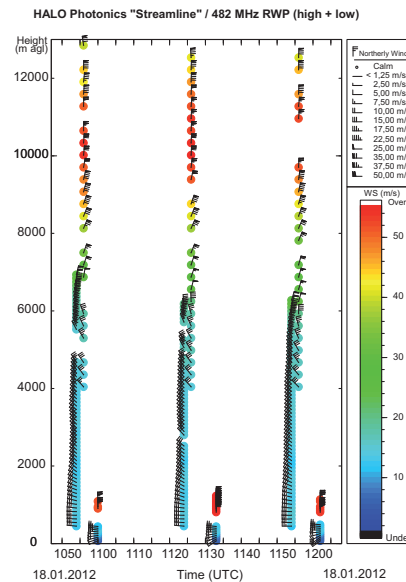


**Figure 12.** Comparison of three pairs of wind profiles obtained from Doppler lidar measurements and wind profiler measurements on January 08, 2012 respectively, at the three different times (time slots) around 11:00 UTC, 11:30 UTC and 12:00 UTC on January 18, 2012. For each time the wind profiler measurements are to the left and the Doppler lidar measurements are to the right. It can be observed that there are huge differences between the The wind profiler measurements around 1 km height. In particular are obtained for two different modes, the winds measured with the Doppler lidar seem to be implausible due to the untypical strong wind speeds of about  $60 \text{ m s}^{-1}$ . If one takes e. a closer look to the (high mode) lower one providing wind profiler measurements from 450 m up to 9380 m and taking a higher one providing additional measurements from about 4000 m up to 13000 m. The colors indicate the pulse repetition frequency ( $PRF = 15 \text{ kHz}$ ) wind speed, see also Tab. ??) into account which defines the maximum measurement height  $Z_{max} = 10 \text{ km}$  for wind barbs give further information on the Doppler lidar used in this study these huge differences can be explained as follows. The wind profiler (high mode) measures winds of about  $60 \text{ m s}^{-1}$  in heights around 11 km direction. Also the Doppler lidar measures these winds but due to  $Z_{max} = 10 \text{ km}$  the calculation of the range is incorrect and the signals from the backscattering targets higher than 10 km are erroneously allocated to heights around 1 km.